Impact of Tether Length on Bone Mineral Affinity of Protein–Bisphosphonate Conjugates

Sébastien A. Gittens,[1,2] Pavel I. Kitov,[3] John R. Matyas,[5] Raimar Löbenberg,[1] and Hasan Uludağ[1,2,4,6]

Received October 1, 2003; accepted December 24, 2003

Purpose. To determine the effect of tether length on bone mineral affinity of fetuin–bisphosphonate conjugates.

Methods. 1-Amino-1,1-diphosphonate methane (aminoBP) was conjugated onto the lysine residues of fetuin by using five different cross-linkers that varied in length. Both the conjugation efficiency (i.e., the number of aminoBPs per protein) as well as molecular dynamics modeling of the resulting conjugates were assessed. Furthermore, the *in vitro* and *in vivo* bone mineral affinity of the conjugates were compared to one another.

Results. The tethers, whose extended lengths varied from 5.7 to ~136 Å, were effective in conjugating aminoBP onto fetuin. Molecular dynamics modeling revealed an inverse relationship between tether length and the maximal radial density of the pendent ligand. The capacity of the conjugates to bind to various bone matrices *in vitro* differed significantly, as aminoBPs tethered onto fetuin via shorter cross-linkers afforded a superior affinity for various mineral matrices than those tethered via longer cross-linkers. Results from the *in vivo* mineral implantation studies corroborated the *in vitro* findings, as higher binding was achieved with the shorter conjugates. Thus, the binding capacities of the conjugates paralleled the maximal radial densities of the pendent ligands.

Conclusions. The use of any of the chosen cross-linkers was feasible in conjugating aminoBP onto fetuin. Maximal mineral binding of the fetuin–aminoBP conjugates, however, was typically achieved using the shorter cross-linkers.

KEY WORDS: bisphosphonates; bone binding; heterobifunctional crosslinkers; hydroxyapatite affinity; tether length.

INTRODUCTION

To enable the use of osteogenic growth factors to promote systemically the regeneration of bone for clinical indications such as osteoporosis, these proteins must be targeted to skeletal tissues in order to circumvent the extraskeletal effects they may elicit upon parenteral administration (1). A promising approach to delivering these proteins to bone is by conjugating bisphosphonates (BPs), pyrophosphate analogs with an inherently high affinity for the hydroxyapatite (HA) mineral content of bone, directly onto them via a tether (2–5). In designing BP–protein conjugates, the inherent affinity of the BP to bone mineral, as well as the nature (i.e., size and molecular structure) of the BP and tether are ultimately expected to influence the bone affinity ultimately imparted onto the conjugate (6). We have previously shown that the conjugation of 1-amino-1,1-diphosphonate methane (aminoBP) onto the carbohydrate moieties of bovine fetuin using 4-(maleimidomethyl) cyclohexane-1-carboxyl-hydrazide (MMCCH) was feasible. This process of conjugation enhanced protein affinity for various bone matrices *in vitro* (7). When compared to conjugates that have aminoBP covalently attached onto the lysine residues of fetuin using succinimidyl-4-(*N*-maleimidomethyl)-cyclohexane-1-carboxylate (SMCC), however, the affinity of the MMCCH-conjugates was found to be superior than that of the SMCC-conjugates. We postulated that the steric interference mediated by the amino acids adjacent to the linkage site may have accounted for the difference in the capacity of the SMCC conjugates to bind to various mineral matrices. Alternatively, the carbohydrate moieties may have afforded a greater range of motion to facilitate the interaction between the conjugated aminoBPs and mineral matrices (7). Indeed, these observations were consistent with theoretical models in which binding between receptor–ligand pairs hindered by steric interference are improved by increasing tether length (6,8) as well as with experimental observations in liposomal targeting (9–13), gene delivery (14,15), immunosorbent assays (16,17), and the functionalization of cell-adhesive surfaces (18). As a result, it was expected that increasing the tether length of the BP conjugates would enhance aminoBP-mediated conjugate binding to mineralized matrices.

This study was performed in order to explore the influence of the tether on the mineral affinity of the BP-conjugates. Several conjugates with varying tether lengths have been prepared, and their mineral affinity was explored in *in vitro* binding assays and in an *in vivo* implant model. In conjunction with experimental studies, molecular dynamics modeling was performed to better characterize the influence of various cross-linkers on the bone affinity of the conjugates. The results presented herein are expected to improve the design of future aminoBP–protein conjugates by providing insight into ways of optimizing the conjugate affinity to bone.

[1] Faculty of Pharmacy & Pharmaceutical Sciences, University of Alberta, Edmonton, Alberta, Canada T6G-2G6.
[2] Department of Biomedical Engineering, Faculty of Medicine & Dentistry, University of Alberta, Edmonton, Alberta, Canada T6G-2G6.
[3] Department of Chemistry, Faculty of Science, University of Alberta, Edmonton, Alberta, Canada T6G-2G6.
[4] Department of Chemical & Materials Engineering, Faculty of Engineering, University of Alberta, Edmonton, Alberta, Canada T6G-2G6.
[5] Department of Cell Biology & Anatomy, Faculty of Medicine, University of Calgary, Alberta, Canada T2N 4N1.
[6] To whom correspondence should be addressed. (e-mail: hasan.uludag@ualberta.ca)

ABBREVIATIONS: aminoBP, 1-Amino-1,1-diphosphonate methane; BP, bisphosphonates; DMF, *N,N*-dimethylformamide; HA, hydroxyapatite; 2-IT, 2-iminothiolane; MANS, α-maleimidoacetic acid-*N*-hydroxysuccinimide; MBNS, maleimidobutyric acid-*N*-hydroxysuccinimide; MMCCH, 4-(maleimidomethyl) cyclohexane-1-carboxyl-hydrazide; MD, molecular dynamics; MW, molecular weight; NHS-PEG-MAL, *N*-hydroxysuccinimide-polyethylene glycol-maleimide; SDS, sodium dodecyl sulfate; SMCC, succinimidyl-4-(*N*-maleimidomethyl)-cyclohexane-1-carboxylate; LC-SMCC, succinimidyl-4-(*N*-maleimidomethyl)cyclohexane-1-carboxy-(6-amidocaproate); TCDG, 1,3,4,6-tetrachloro-3α,6α-diphenylglycouril; TCA, trichloroacetic acid.

0724-8741/04/0400-0608/0 © 2004 Plenum Publishing Corporation

MATERIALS AND METHODS

Materials

Succinimidyl-4-(*N*-maleimidomethyl)cyclohexane-1-carboxylate (SMCC), succinimidyl-4-(*N*-maleimidomethyl)-cyclohexane-1-carboxy-(6-amido-caproate) (LC-SMCC), α-maleimidoacetic acid-*N*-hydroxysuccinimide (MANS), and maleimidobutyric acid-*N*-hydroxysuccinimide (MBNS) were acquired from Molecular Biosciences (Boulder, CO, USA). *N*-hydroxysuccinimide-polyethylene glycol-maleimide (NHS-PEG-MAL) with molecular weight (MW) of 2300 Da was from Nektar Therapeutics (Huntsville, AL, USA). Bovine fetuin (lot #59H7616), 2-iminothiolane (2-IT), bovine adult serum, trichloroacetic acid (TCA), and 1,3,4,6-tetrachloro-3α,6α-diphenylglycouril (TCDG) were obtained from Sigma Aldrich (St. Louis, MO, USA). Precast 4–20% LongLife polyacrylamide gels were from Gradipore (Frenchs Forest, NSW, Australia), whereas $Na^{125}I$ (in 0.1 M NaOH) was obtained from Perkin Elmer (Wellesley, MA, USA). 0.9% NaCl was from Baxter Corporation (Toronto, ON, Canada). *N,N*-dimethylformamide (DMF) was from Caledon Laboratories (Georgetown, ON, Canada). The Spectra/Por dialysis tubing with MW cutoff of 12–14,000 Da was acquired from Spectrum Laboratories (Rancho Dominguez, CA, USA). The SDS-glycine sample buffer for electrophoresis was prepared as previously described (7). The SDS-PAGE running buffer was prepared by the addition of 2.9% (w/v) Trizma Base, 14.4% (w/v) glycine, and 1.0% (w/v) SDS in deionized water. Metofane (methoxyflurane) was obtained from Janssen Inc. (Toronto, ON, Canada). The Pro-Osteon 200HA implants, which were coralline hydroxyapatite disks (10 mm in diameter × 4 mm in thickness) with porous three-dimensional microarchitecture similar to that of cortical bone (19), were kindly donated by Interpore Cross International (Irvine, CA, USA).

AminoBP Conjugation onto Fetuin

Conjugations by SMCC, LC-SMCC, MANS, MBNS, and NHS-PEG-MAL, heterobifunctional cross-linkers with $–NH_2$ and –SH reactive groups, were performed according to a previously published procedure (7). Briefly, fetuin (15 mg/ml in 0.1 M phosphate buffer) was incubated for 2.5 h with up to 15 mM of one of the cross-linkers, which was initially dissolved in DMF at a concentration of 45 mM. Separately, aminoBP was thiolated by incubating equal volumes of aminoBP (80 mM in 0.1 M phosphate buffer) with 2-IT solution (40 mM in 0.1 mM phosphate buffer) for 2.5 h. The product from this reaction was then directly added to the cross-linker–reacted fetuin in equal volumes and incubated for 2.5 h at room temperature. To remove the unreacted reagents (i.e., aminoBP, 2-IT, thiolated aminoBP, and cross-linker), the conjugates were thoroughly dialyzed against 0.1 M carbonate buffer (x3) and deionized water (x2).

Analysis of the Conjugates

After dialysis, protein concentrations were determined using the Bradford Protein Assay (20) as follows: a 50-μl sample was added to 1 ml of the protein reagent, which consisted of 0.01% (w/v) Coomassie Blue R-250, 4.7% (w/v) ethanol, and 8.5% (w/v) phosphoric acid. The sample's absorbance was subsequently determined at 595 nm. A phosphate assay, which was modified from that described by Ames (21), was then used to determine aminoBP concentration of the samples (7). The aminoBP concentrations of the protein samples were used in combination with the results from the protein assay to yield the number of aminoBPs conjugated onto fetuin (mol:mol ratio). Gel electrophoresis was used to determine whether inadvertent protein–protein cross-linking occurred during the process of conjugation. As the molecular weight of fetuin is 48.4 kDa, protein–protein cross-linking would have manifested itself as ≥100 kDa protein bands on the gels. Approximately 10 μg of protein sample was mixed with an SDS-glycine sample buffer and loaded onto a 4–20% Tris-HCl polyacrylamide gel. The samples were run at 150 V for 1.5 h in an SDS-glycine running buffer. The gels were then stained overnight using a Coomassie Blue R-250 (0.1% w/v Coomassie Blue R-250 in 10:10:80 = methanol:acetic acid: deionized water), destained, and scanned on a flat-bed scanner.

Molecular Dynamics Modeling of the Conjugates

Molecular dynamics (MD) modeling of the conjugates was used to correlate the conformational properties of the linkers with aminoBP ligand moieties to the fetuin conjugates' capacity to bind to various bone matrices. All modeling was performed using *Insight-II* suite of software programs (Molecular Simulations Inc, San Diego, CA, USA) on a Silicon Graphics Octane-2 workstation. The structures to be modeled (Fig. 1), which are subsequently referred to as pendent ligands, were generated using the standard fragment library in *Biopolymer* block. The aminoBP ligands were modeled as both charged and uncharged moieties. Individual pendent ligands were simulated without the influence of protein and other ligands. Consistent valence forcefield (CVFF) potentials were automatically assigned followed by manual correction where necessary; after the formal charges for all atoms were set to zero, the partial charges were automatically generated. Free energies for all structures were sufficiently minimized prior to the initiation of MD modeling. The dielectric constant was set to 80 and the temperature to 1000 K (a temperature selected for simulation in order to accelerate the collection of a representative set of structural configurations). Each MD experiment, except for the NHS-PEG-MAL cross-linker, was conducted for 2.5 ns (with a step of 1 fs), with trajectories being sampled after every 250 steps. In the case of NHS-PEG-MAL, the configurational space was explored for 10 ns and every 1000th frame was sampled. For individual pendent ligands, the distances (also known as the end-to-end separation) between lysine's α-carbon and the aminoBP's central carbon (separating the two phosphonate moieties) were measured from each of the 10,000 frames obtained from the simulations. Histograms with a step of 0.5 Å were subsequently generated to determine probability density. The radial density distribution was calculated by normalizing the probability density by the volume enclosed by two hemispheres with the center at the attachment point and radii R and R-0.5 Å (as described in Ref. 24).

Assessment of Conjugate Mineral Affinity

Preparation of Radioiodinated Conjugates

Binding was assessed by using ^{125}I-labeled proteins. In tubes previously coated with TCDG (200 μl of 20 μg/ml

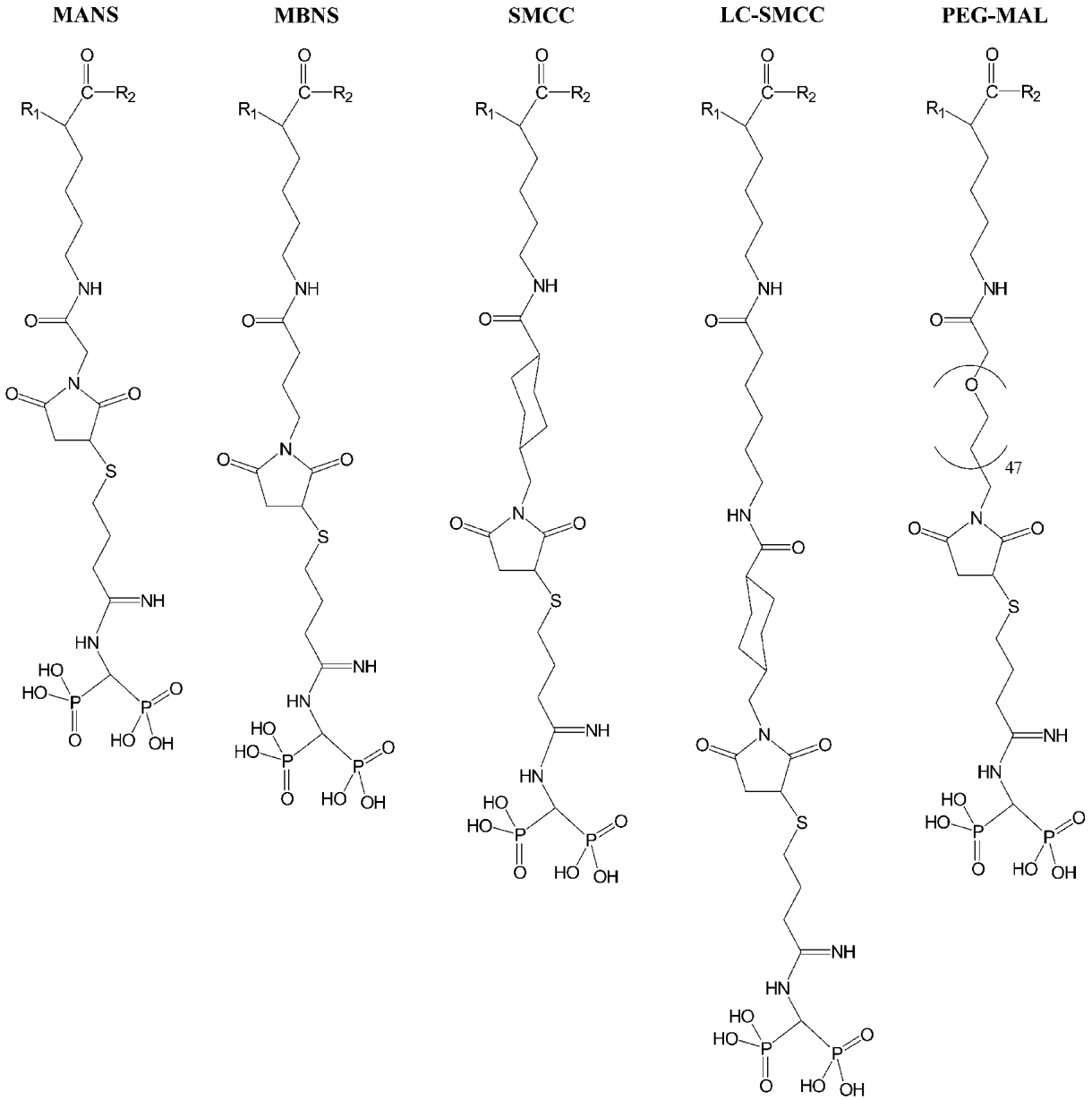

Fig. 1. A representation of the MANS-, MBNS-, SMCC-, LC-SMCC-, and NHS-PEG-MAL-conjugates pendent ligands. The substituents R_1 and R_2 at the lysine moiety represent preceding and following amino acid residues in the peptide chain. In the structures that were used in MD simulations, R_1 = $-NH_2$ and R_2 = –H. The extended conformational length of listed heterobifunctional cross-linkers themselves, from the maleimide moiety up to but excluding the succinimide moiety, were 5.7, 10.2, 11.6, 16.1, and ~136 Å (6), respectively.

TCDG in chloroform), 10 μg of protein was added to 50 μl of 0.1 M phosphate buffer (pH 7.4) and 10 μl of 0.01 mCi of $Na^{125}I$ (in 0.1 M NaOH). After reacting for 20 min, free ^{125}I was separated from the radiolabeled protein via dialysis against 0.05 M phosphate buffer. After precipitating an aliquot of the samples with 20% TCA, it was confirmed that all iodinated samples contained <5% free ^{125}I.

In vitro Mineral Binding

The preparation of HA has previously been described (2). The radiolabeled proteins were added to cold protein to give a radioactive count of 10^6 cpm at a 0.1 mg/ml protein concentration. Along with 175 μl of 50% bovine adult serum (diluted with 0.9% saline), 25 mg of normal bone or 5 mg of HA was added to microcentrifuge tubes. This serum-containing binding medium was used because it better represented physiological conditions than phosphate buffers (7). After periodical shaking during a 3 h period, the samples were centrifuged. The supernatant was collected, and the pellet, consisting of the mineral matrix, was washed with the binding buffer used, then re-centrifuged. This washing procedure was then repeated twice more, and the collected supernatant from each of these steps was subsequently counted separately by a γ-counter (Wallac Wizard 1470, Turku, Finland). Matrix affinity, expressed as percentage matrix binding, was calculated as follows: 100% × (counts in matrix pel-

let) ÷ [(counts in matrix pellet) + (counts in supernatants)]. All binding was assessed in duplicate.

The affinity of the conjugates to the mineral matrix used for implantation (i.e., Pro-Osteon) was also determined *in vitro*. A 50-μl aliquot, containing 2.5×10^5 cpm of radiolabeled conjugate along with 0.1 mg/ml cold protein, was initially applied to each autoclaved Pro-Osteon disk. Following a 10-min incubation period, the disks (two per group) were washed thoroughly (five times) using 50% bovine adult serum in saline. The supernatants collected from each of the washes, along with the implants themselves, were quantified separately using a γ-counter. The affinities that the conjugates exhibited for the implants were calculated using the "matrix affinity" formula described above.

In vivo HA-based Matrix Binding

Two-month-old female Sprague-Dawley rats were purchased from Charles River Laboratories (Quebec City, PQ, Canada). Rats were acclimated until 3 months of age under standard laboratory conditions (23°C, 12 h of light/day) prior to the beginning of the study. While maintained in pairs in sterilized cages, rats were provided standard commercial rat chow and tap water *ad libitum* for the duration of the study. All procedures involving the rats were approved by the Animal Welfare Committee at the University of Alberta (Edmonton, Alberta, Canada).

For assessing conjugate affinity to bone *in vivo,* powdered HA was considered unsuitable due to the difficulty associated with recovering the particulate HA matrix following implantation. Consequently, Pro-Osteon disks, which are clinically used for bone implantation, were used. The disks used for *in vivo* implantation were prepared essentially as described above. The initial counts in the implant were determined before implantation. Once rats were anesthetized with Metofane, two Pro-Osteon disks were implanted subcutaneously into bilateral ventral pouches in each rat (n = 2 rats per conjugate group). Three days following implantation, the rats were asphyxiated with CO_2. The radioactivity associated with the excised implants and the soft tissue surrounding the implant was quantified separately using a γ-counter. The degree of protein retention, expressed as a percentage of the implanted dose, was calculated as follows: 100% × [(final counts in implant) ÷ (initial counts in implant)].

Statistics

Significant differences ($p < 0.05$) in conjugate binding to the Pro-Osteon disks were determined by Tukey post-hoc comparison. Linear regression was also used in the analysis of the data. All statistics was done using SPSS for Windows 11.0.1 (SPSS Inc., Chicago, IL, USA).

RESULTS

AminoBP Conjugation to Fetuin

Conjugation of aminoBP onto the lysine $-NH_2$ moieties of fetuin was carried out using MANS, MBNS, SMCC, LC-SMCC, and NHS-PEG-MAL. While keeping thiolated aminoBP concentrations at 20 mM, increasing the concentration of cross-linker during the process of conjugation led to a concentration-dependent increase in the number of aminoBPs attached onto fetuin (Fig. 2). The maximal conjugation efficiency using MANS, MBNS, SMCC, LC-SMCC, and NHS-PEG-MAL were 9.7, 15.0, 23.0, 17.8, and 22.1 aminoBPs/fetuin, respectively. These were significantly higher than their respective controls (i.e., fetuin reacted with 0 mM cross-linker and 20 mM thiolated aminoBP prepared for each conjugate), which had an average of 1.8 ± 0.5 aminoBPs/fetuin. Each cross-linker used, regardless of its length, successfully facilitated the conjugation of aminoBP onto fetuin.

Corresponding to the degree of conjugation, gel electrophoresis indicated that there were slight upward shifts in the intensity of conjugates' bands relative to native fetuin's band at 48.4 kDa—especially with the larger molecular weight cross-linked conjugates such as LC-SMCC and NHS-PEG-MAL. No visible bands at the ~100-kDa region, however, presented themselves (data not shown). These results confirmed that aminoBP conjugation had indeed occurred (as was especially evident with the use of the larger molecular weight cross-linkers) and that the occurrence of protein–protein cross-linking was insignificant for all cross-linkers.

Molecular Dynamics Modeling of the Conjugates

MD modeling was used to characterize the conformational behavior of linker structures containing pendent aminoBP ligand moieties. As illustrated in Fig. 3, the calculated maximal probability densities as well as the radial distribution profiles were inversely related to the length of cross-linkers used. Possessing fewer potential structural permutations, aminoBPs tethered onto fetuin using shorter cross-linkers (i.e., MANS, MBNS, and SMCC) were more likely to be within a shorter distance of the protein core, which consequently induced a greater density of the pendent ligand than those tethered using longer cross-linker (i.e., LC-SMCC and NHS-PEG-MAL). A small increase in the MANS and MBNS pendent ligands' maximal probability density was seen (from a maximal density of ~0.038 to 0.057 and 0.048, respectively) when the aminoBP moiety of the pendent ligands were mod-

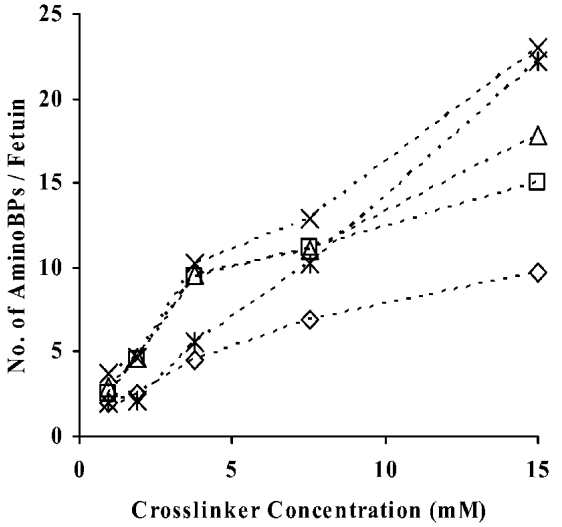

Fig. 2. The conjugation efficiency of aminoBP onto fetuin. As the concentrations of MANS (◊), MBNS (□), SMCC (X), LC-SMCC (Δ), and NHS-PEG-MAL (*) increased, the subsequent number of conjugated aminoBPs rose linearly (r^2 = 0.961, 0.859, 0.975, 0.987, and 0.996, respectively).

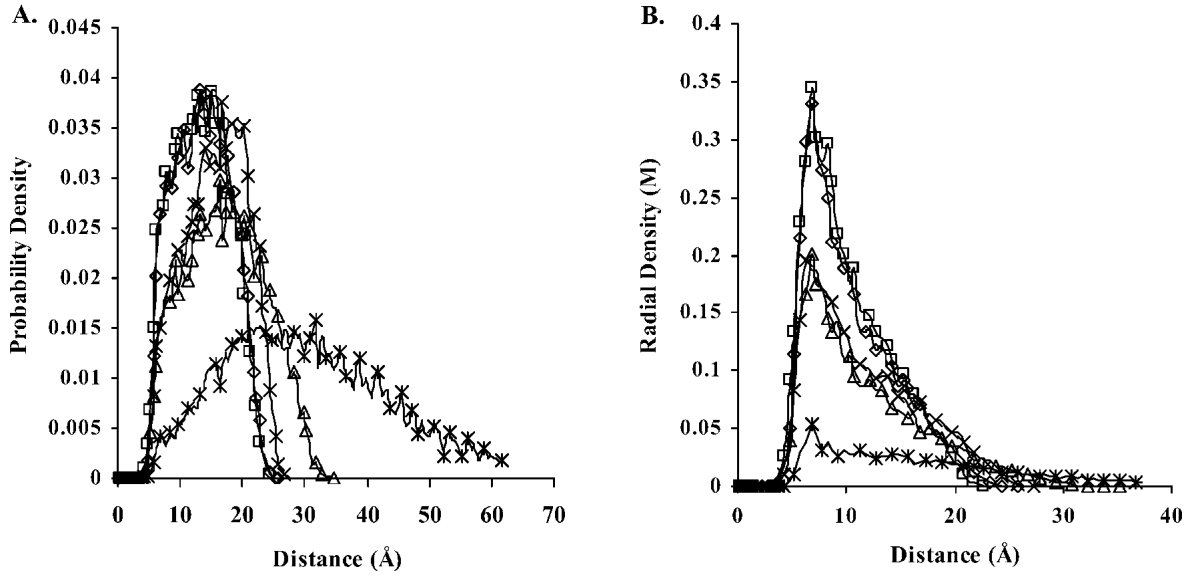

Fig. 3. (A) The probability density and (B) the radial density distribution of the charged MANS (◊), MBNS (□), SMCC (X), LC-SMCC (Δ), and NHS-PEG-MAL (*) pendent ligands. In each case, maximal probability density and radial density were inversely proportional to the size of the tether used.

eled uncharged. Otherwise, no other noticeable differences in either the pendent ligands' radial or probability densities were observed between modeling the charged or uncharged aminoBP moieties.

Conjugate Binding to Bone and HA Matrices *In vitro*

The MANS, MBNS, SMCC, and LC-SMCC conjugates exhibited a binding to HA that was aminoBP-dependent: samples with low conjugation efficiency had ~20% binding, whereas samples with high conjugation efficiency had >50% binding (Fig. 4). The binding efficiency for each group of conjugates differed significantly; however, the conjugates whose aminoBPs were tethered onto fetuin via shorter cross-linkers, namely the MANS, MBNS, and SMCC, bound to the synthetic mineral matrix more tenaciously (with a maximum binding of 63.8%, 66.1%, and 74.0%, respectively) than the longer LC-SMCC conjugates, which exhibited reduced binding (maximum binding of 45.6%). Despite its relatively high conjugation efficiency, the NHS-PEG-MAL conjugate binding to HA diminished significantly in a manner proportional to the number of aminoBPs conjugated onto fetuin. These conjugates exhibited the weakest capacity to bind to HA relative to any of the other conjugation products. In comparison, binding of control fetuin to HA was significantly lower (averaging 13.3 ± 4.8%). These results also corroborated the fact that HA binding was mediated by the conjugated aminoBP.

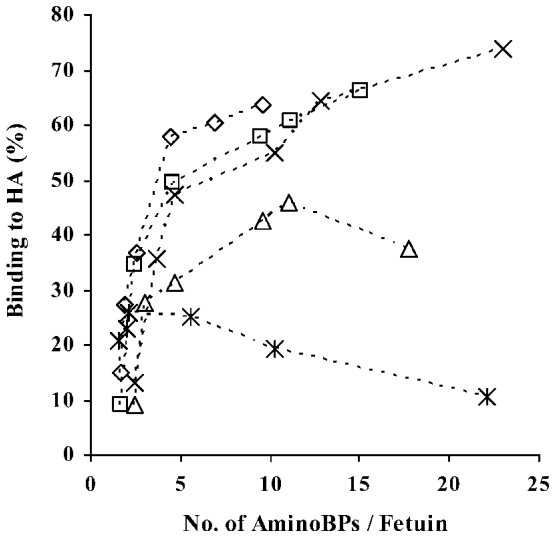

Fig. 4. The MANS (◊), MBNS (□), SMCC (X), LC-SMCC (Δ), and NHS-PEG-MAL (*) conjugates' capacity to bind to HA in 50% bovine adult serum. The conjugates synthesized using the MANS, MBNS, and SMCC tethers bound to HA more extensively than those synthesized with LC-SMCC and NHS-PEG-MAL.

To further characterize conjugate binding to HA, binding isotherms for each group of conjugates were generated. The conjugate samples chosen for these studies were those containing ~10 aminoBPs/fetuin. As previously observed, the MANS, MBNS, and SMCC conjugates exhibited superior binding to HA, followed by the LC-SMCC conjugates and the NHS-PEG-MAL conjugates (Fig. 5).

Using the same conjugates as above (i.e., ~10 aminoBPs/fetuin), the effect of modulating bovine adult serum concentration on conjugate binding to HA was subsequently determined. As shown in Fig. 6, all conjugates, even the NHS-PEG-MAL conjugates, exhibited exceptional binding to HA in the absence of serum (in saline). As the concentration of adult bovine serum increased, the propensity of all conjugates to bind to HA decreased. This reduction in binding, however, was not uniform, as the conjugates with the longest cross-linkers (i.e., LC-SMCC and NHS-PEG-MAL) were more adversely affected by the increasing competitive-nature of the binding media. These results reflected trends found in the previous binding results: aminoBPs tethered onto fetuin via longer cross-linkers afforded the poorest conjugate binding to HA.

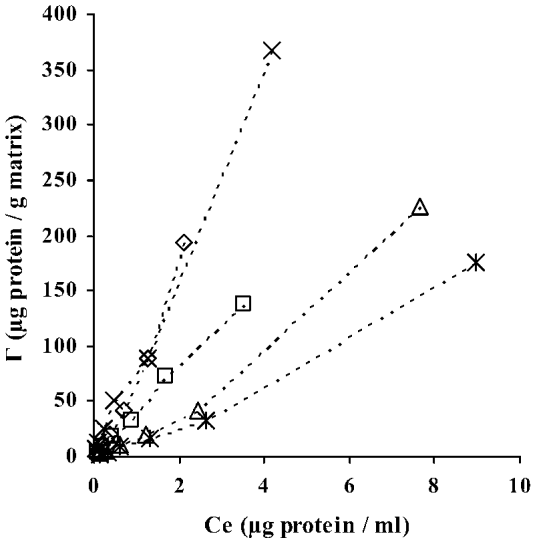

Fig. 5. Binding isotherms of the MANS (◊), MBNS (□), SMCC (X), LC-SMCC (Δ), and NHS-PEG-MAL (*) conjugates with HA. Conjugate concentrations were serially diluted 2-fold from a maximum 10^6 cpm at 0.1 mg/ml and the resulting conjugate binding was expressed as C_e (the equilibrium concentration after the 3 h binding period) vs. Γ (the amount of bound protein per gram of HA). The slopes and corresponding correlation coefficient (r^2) values for the each of the conjugates are: 91.7, 0.976; 39.5, 0.997; 86.0, 0.992; 30.0, 0.981; and 19.7, 0.989; respectively.

Conjugate Retention to HA-Implants *In vivo*

Given the similar binding profiles of the MANS, MBNS, and SMCC conjugates, the MBNS conjugate was chosen to represent the group of shorter cross-linkers in the *in vivo* experiments. Using 50% bovine adult serum, the *in vitro* affinity that native fetuin had for the Pro-Osteon implants (26.0 ± 5.9%) was lower than the MBNS, LC-SMCC, and NHS-PEG-MAL conjugates (82.5 ± 1.9%, 83.2 ± 3.5%, and 46.7 ± 1.7%, respectively, Fig. 7A). In contrast to the HA binding results, the MBNS conjugate's mineral affinity was not different to that of the LC-SMCC conjugate. Following 3 days of implantation, all conjugates exhibited higher affinity to the Pro-Osteon matrix compared to unconjugated fetuin ($p < 0.02$). Conjugate retention to the soft tissue surrounding the implant, however, was negligible (<0.2% of the dose implanted on average). This was indicative of rapid clearance of the released protein from the site of implantation. The affinity of the NHS-PEG-MAL conjugate was lower than both the MANS and LC-SMCC conjugates. Following their *in vitro* binding profiles to Pro-Osteon, the MBNS and LC-SMCC conjugate retention in Pro-Osteon disks were significantly greater than the unconjugated fetuin or the NHS-PEG-MAL conjugates ($p < 0.0005$ and $p < 0.0005$, respectively) (Fig. 7B). A plot of conjugate binding to Pro-Osteon *in vitro* vs. *in vivo* (not shown) yielded a strong correlation ($r^2 = 0.999$) that was statistically significant ($p < 0.0005$).

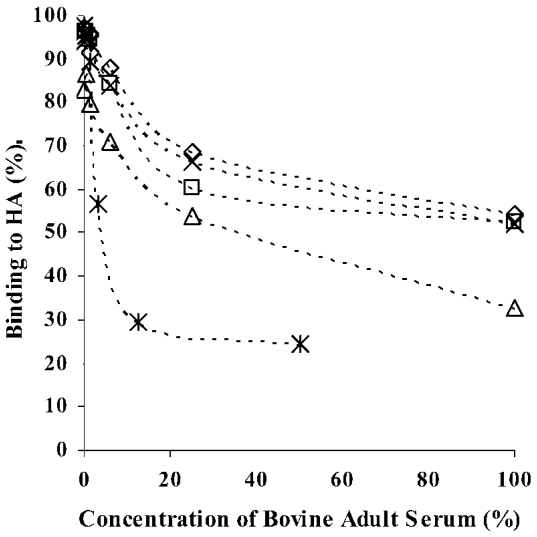

Fig. 6. Modulating bovine adult serum concentration affects the MANS (◊), MBNS (□), SMCC (X), LC-SMCC (Δ), and NHS-PEG-MAL (*) conjugates' capacity to bind to HA. Binding of the LC-SMCC and NHS-PEG-MAL conjugates were more adversely affected by the increasing serum concentrations than the MANS, MBNS, and SMCC conjugates.

DISCUSSION AND CONCLUSIONS

It was the goal of this study to elucidate the effect of tether length on aminoBP–fetuin conjugate affinity for various mineral matrices. Fetuin was chosen as a model protein in this study due several reasons, including our desire to directly compare the current results to our previous studies (7); the already existing information on fetuin's binding capacity to mineralized matrices *in vitro*; and fetuin's important role in modulating bone growth and remodeling (23) as well as ectopic calcification *in vivo* (24). Here, we elected to conjugate aminoBP onto fetuin's protein core so that by varying tether length, the resulting conjugates could meet, if not exceed, the aforementioned superior affinity imparted by aminoBP conjugation onto fetuin's carbohydrate groups (7). Consequently, the five cross-linkers used (i.e., MANS, MBNS, SMCC, LC-SMCC, and NHS-PEG-MAL) were chosen based primarily on their varying lengths. The results described suggest that irrespective of the cross-linker's length, each was capable of facilitating the conjugation of aminoBP directly onto fetuin in a concentration-dependent manner. Conjugation efficiency, however, appeared to be dependent on the cross-linker length as the shorter tethers (namely MANS and MBNS) were less efficient in conjugating aminoBPs onto fetuin than the longer counterparts. As previously shown (2–4,7), the data presented herein suggests that the mineral binding was indeed mediated by aminoBP. Similar to previous observations with the SMCC conjugates (7), a saturable binding kinetics was observed with the MANS, MBNS, SMCC, and LC-SMCC conjugates. At low conjugation efficiencies (i.e., <4 aminoBPs/fetuin), the extent of HA binding was proportional to the number of conjugated aminoBPs. As the conjugation efficiency was increased, however, the aminoBPs tethered onto fetuin using the shorter cross-linkers (i.e., MANS, MBNS, and SMCC) imparted a higher HA affinity than those tethered using the longer cross-linkers (i.e., LC-SMCC and NHS-PEG-MAL). In addition to these results, a similar pattern emerged from the experiments that explored the effects of modulating conjugate (Fig. 5) and competing serum concentrations (Fig. 6) on HA binding. Unlike HA, however, Pro-Osteon did not reveal any differences in affinity between the conjugates derived from the use of either MBNS or LC-SMCC. The PEG-linked conjugates, however, were again inferior in mineral

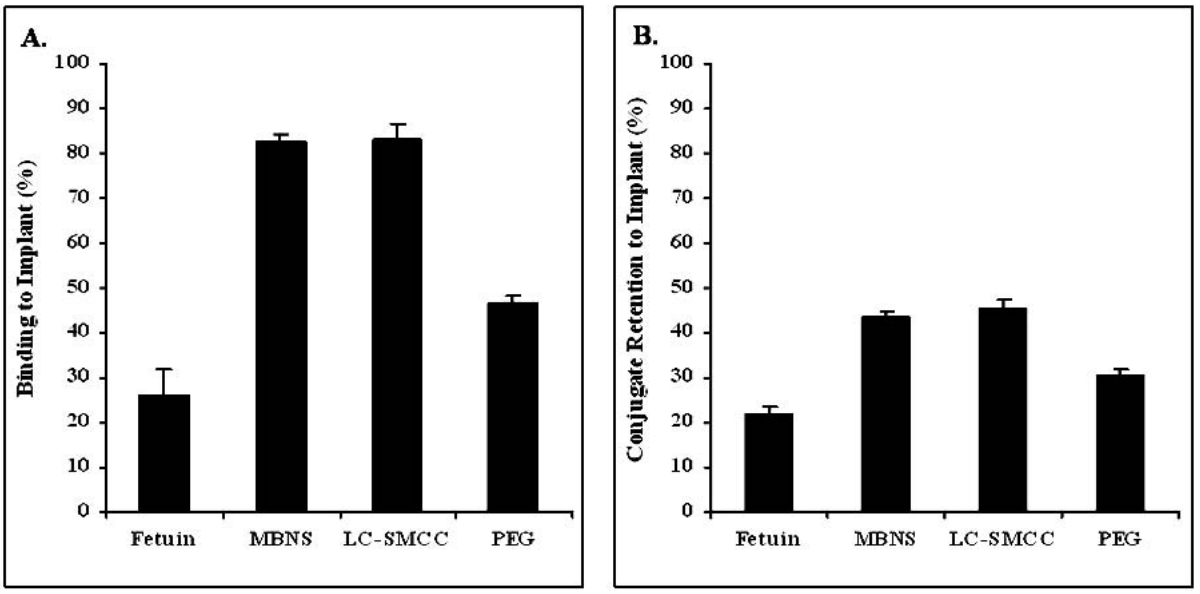

Fig. 7. Mean ± SD of the capacity of native fetuin and the MBNS, LC-SMCC, and NHS-PEG-MAL conjugates (A) to bind to Pro-Osteon *in vitro* as well as (B) their retention in the biomaterial 3 days after implantation *in vivo*. In both cases, the binding of the MBNS and LC-SMCC conjugates was superior to that of the NHS-PEG-MAL conjugates and even more so the native fetuin.

binding. We do not currently know which matrix properties were responsible for the binding differences between the HA synthesized in-house and the commercially-available Pro-Osteon, but the binding pattern to the latter matrix was consistent both *in vitro* and *in vivo*.

Similar to our findings, Hirabayashi *et al.* had observed that an increase in tether length from 1 to 10 methylene groups between carboxyfluorescein (an organic molecule much smaller than proteins) and a BP resulted in a nearly 10-fold *decrease* in skeletal targeting upon the compounds' intravenous administration (25). They postulated that this decrease in targeting was due to a corresponding increase in the molecules' hydrophobicity, as determined through theoretical calculations of the compounds' octanol/water partition coefficient. (It should be noted that the mineral affinities of their conjugates were not assessed *in vitro*.) The NHS-PEG-MAL tether used in this study, which is significantly more hydrophilic than the methylene-based tethers used in the study of Hirabayachi *et al*., resulted in a reduction in conjugate mineral affinity. Consequently, it is postulated that tether hydrophobicity is unlikely to be the underlying factor responsible for the reduction in the mineral affinity associated with increased tether lengths.

The strength of tethered aminoBP–HA binding is expected to depend primarily on the number of aminoBP ligands incorporated onto the conjugate, the strength of the individual aminoBP–HA interactions, and the surface area of HA available for the interactions (6). Because the amount of mineral matrix (and thus the interacting surface) remained constant throughout each experiment, binding of conjugates with comparable degree of conjugation efficiency to HA should primarily rely on the strength of individual pendent ligand–HA interactions. Because the same ligand was used throughout this study (i.e., aminoBP), it is reasonable to assume that the intrinsic binding energies did not vary among conjugates. On the other hand, the probabilities of aminoBP–HA interaction and the corresponding entropic terms should differ according to the effective concentration (i.e., radial density) of aminoBP at the HA surface. Therefore, the end-to-end separation between pendent ligand and protein at the maximum radial density corresponds to the distance most favorable for conjugate–HA interaction and represents the equilibrium distance between the pendent ligand and the attachment point in the bound state. Using a library of oligosaccharide ligands, the magnitude of the radial density at the equilibrium distance was previously shown to be proportional to the binding constant of the interacting species (22). Various tethers used in forming this oligosaccharide library were ranked according to their apparent binding efficiencies (22) and validated in an experimental setup. The radial density of our pendent ligands were in agreement with our experimental observations of the conjugates' capacity to bind to bone mineral and have provided a further validation for the usefulness of this computational approach in the design of therapeutic agents constructed from the linkage of two separate molecules, where one of these molecules was intended to impart a target affinity. Based on this framework, it might be suitable to design optimal tethers *in silico*, rather than empirically attempting to identify suitable tethers in an experimental system. As an increase in tether length would enable a ligand to escape the adverse effects of steric hindrance exerted from neighboring amino acids, it can be inferred from these data that steric effects did not influence aminoBP binding onto HA. Consequently, we postulate that steric hindrance (originating from the protein) was probably not the likely reason for the significant difference observed between aminoBP conjugated onto fetuin's protein core and its carbohydrate residues. It may be possible, however, that steric hindrance elicited by the coiled, and thus relatively bulky, longer tethers (especially the PEG-based linker) may have adversely affected the conjugated aminoBP's capacity to bind to HA. Perhaps other interactions between HA and the protein's functional groups (as suggested by Refs. 26 and 27) contributed to additional binding that helped stabilize and/or im-

prove aminoBP-mediated conjugate binding. Because longer tethers retain the protein at a distance from the surface of HA, this too might be why longer tether lengths are less effective in facilitating conjugate–HA binding.

The results from the Pro-Osteon implantation study suggest that the mineral affinity imparted by the conjugation of aminoBP onto fetuin leads to a significant degree of protein retention to the HA-based biomaterial over nonconjugated protein. Given that the retention of the osteogenic proteins [i.e., those capable of inducing bone formation such as several members of the BMP family (1)] correlates directly with the degree of bone formation they elicit (28), these implications are significant as they suggest that HA-based implants, which are used in numerous clinical applications, may be applied with BP-conjugated osteogenic proteins. Furthermore, these results are of clinical relevance as Pro-Osteon itself has been used as a bone substitute in numerous orthopedic, ophthalmologic, and maxillofacial applications (19). It is thought that this BP-based delivery system may improve the performance of such biomaterials by improving their osteoconductivity as well as afford some degree of osteoinductivity. As previously discussed (7), however, the potential use of BP–protein conjugates is not limited to HA-based implants. In fact, we have previously shown that aminoBP–albumin conjugates exhibit an improved retention when administered intraosseously in a tibial injection animal model—suggesting that our approach may be applicable to promote the regeneration of bone in local defects that do not necessarily require the use of an implant (3).

In summary, this study has shown that a range of cross-linkers could facilitate the conjugation of aminoBP onto fetuin, but the resulting bone mineral affinity for each of these conjugates differed significantly. AminoBPs tethered onto fetuin using the shorter cross-linkers (i.e., MANS, MBNS, and SMCC) imparted a higher affinity than those tethered using the longer cross-linkers (i.e., LC-SMCC and NHS-PEG-MAL). This is the first study to report that the mineral affinity imparted by BP conjugation enhances a protein's retention once implanted by a HA-based biomaterial *in vivo*. The results presented in this report will facilitate improvements in the design of aminoBP–protein conjugates to maximize bone mineral affinity.

ACKNOWLEDGMENTS

This work was financially supported by a Biomedical Engineering Grant from Whitaker Foundation, an Operating Grant from the Canadian Institutes of Health, and Research and Infrastructure Grants from Alberta Heritage Foundation for Medical Research and Canadian Foundation for Innovation. S. A. G. was funded by an Izaak Walton Killam Memorial Scholarship. The authors also wish to thank Dr. K. Bagnall, (Faculty of Medicine and Dentistry, University of Alberta) and Dr. G. R. Wohl (Faculty of Engineering, University of Alberta) for their assistance throughout the course of these studies as well as Dr. M. Borden (Interpore Cross Inc.) for the Pro-Osteon disks.

REFERENCES

1. S. A. Gittens and H. Uludag. Growth factor delivery for bone tissue engineering. *J. Drug Targeting* **9**:407–429 (2001).
2. H. Uludag, N. Kousinioris, T. Gao, and D. Kantoci. Bisphosphonate conjugation to proteins as a means to impart bone affinity. *Biotechnol. Prog.* **16**:258–267 (2000).
3. H. Uludag, T. Gao, G. R. Wohl, D. Kantoci, and R. F. Zernicke. Bone affinity of a bisphosphonate-conjugated protein in vivo. *Biotechnol. Prog.* **16**:1115–1118 (2000).
4. H. Uludag and J. Yang. Targeting systemically administered proteins to bone by bisphosphonate conjugation. *Biotechnol. Prog.* **18**:604–611 (2002).
5. H. Uludag. Bisphosphonates as a foundation of drug delivery to bone. *Curr. Pharm. Des*. **8**:1929–1944. (2002)
6. C. Jeppesen, J. Y. Wong, T. L. Kuhl, J. N. Israelachvili, N. Mullah, S. Zalipsky, and C. M. Marques. Impact of polymer tether length on multiple ligand-receptor bond formation. *Science* **20**: 293:465–468 (2001).
7. S. A. Gittens, J. R. Matyas, R. F. Zernicke, and H. Uludag. Imparting bone affinity to glycoproteins through the conjugation of bisphosphonates. *Pharm. Res.* **20**:978–987 (2003).
8. J. Y. Wong, T. L. Kuhl, J. N. Israelachvili, N. Mullah, and S. Zalipsky. Direct measurement of a tethered ligand-receptor interaction potential. *Science* **275**:820–822 (1997).
9. R. J. Lee and P. S. Low. Delivery of liposomes into cultured KB cells via folate receptor-mediated endocytosis. *J. Biol. Chem.* **269**: 3198–3204 (1994).
10. A. Engel, S. K. Chatterjee, A. Al-arifi, D. Riemann, J. Langner, and P. Nuhn. Influence of spacer length on interaction of mannosylated liposomes with human phagocytic cells. *Pharm. Res.* **20**:51–57 (2003).
11. J. Salord, C. Tarnus, C. D. Muller, and F. Schuber. Targeting of liposomes by covalent coupling with ecto-NAD+-glycohydrolase ligands. *Biochim. Biophys. Acta* **886**:64–75 (1986).
12. C. P. Leamon, D. Weigl, and R. W. Hendren. Folate copolymer-mediated transfection of cultured cells. *Bioconjug. Chem.* **10**:947–957 (1999).
13. C. P. Leamon, S. R. Cooper, and G. E. Hardee. Folate-liposome-mediated antisense oligodeoxynucleotide targeting to cancer cells: evaluation in vitro and in vivo. *Bioconjug. Chem.* **14**:738–747 (2003).
14. C. M. Ward, M. Pechar, D. Oupicky, K. Ulbrich, and L. W. Seymour. Modification of pLL/DNA complexes with a multivalent hydrophilic polymer permits folate-mediated targeting in vitro and prolonged plasma circulation in vivo. *J. Gene Med.* **4**:536–547 (2002).
15. D. V. Schaffer and D. A. Lauffenburger. Optimization of cell surface binding enhances efficiency and specificity of molecular conjugate gene delivery. *J. Biol. Chem.* **273**:28004–28009 (1998).
16. P. Luppa, C. Bruckner, I. Schwab, S. Hauck, S. Schmidmayr, C. Birkmayer, B. Paulus, and H. Hauptmann. 7 alpha-biotinylated testosterone derivatives as tracers for a competitive chemiluminescence immunoassay of testosterone in serum. *Clin. Chem.* **43**: 2345–2352 (1997).
17. C. Bieniarz, M. Husain, G. Barnes, C. A. King, and C. J. Welch. Extended length heterobifunctional coupling agents for protein conjugations. *Bioconjug. Chem.* **7**:88–95 (1996).
18. L. G. Griffith and S. Lopina. Microdistribution of substratum-bound ligands affects cell function: hepatocyte spreading on PEO-tethered galactose. *Biomaterials* **19**:979–986 (1998).
19. J. S. Thalgott, Z. Klezl, M. Timlin, and J. M. Giuffre. Anterior lumbar interbody fusion with processed sea coral (coralline hydroxyapatite) as part of a circumferential fusion. *Spine* **27**:E518–E527 (2002).
20. M. M. Bradford. A rapid and sensitive method for the quantitation of microgram quantities of protein utilizing the principle of protein-dye binding. *Anal. Biochem.* **72**:248–254 (1976).
21. B. N. Ames. Assay of inorganic phosphate, total phosphate, and phosphatases. In E. F. Neufield and V. Ginsburg (eds.), *Methods in Enzymology, Volume VIII, Complex Carbohydrates*, Academic Press, New York, 1966, pp. 115–117.
22. P. I. Kitov, H. Shimizu, S. W. Homans, and D. R. Bundle. Optimization of tether length in nonglycosidically linked bivalent ligands that target sites 2 and 1 of a Shiga-like toxin. *J. Am. Chem. Soc.* **125**:3284–3294 (2003).

23. M. Szweras, D. Liu, E. A. Partridge, J. Pawling, B. Sukhu, C. Clokie, W. Jahnen-Dechent, H. C. Tenenbaum, C. J. Swallow, M. D. Grynpas, and J. W. Dennis. alpha 2-HS glycoprotein/fetuin, a transforming growth factor-beta/bone morphogenetic protein antagonist, regulates postnatal bone growth and remodeling. *J. Biol. Chem.* **277**:19991–19997 (2002).
24. C. Schafer, A. Heiss, A. Schwarz, R. Westenfeld, M. Ketteler, J. Floege, W. Muller-Esterl, T. Schinke, and W. Jahnen-Dechent. The serum protein alpha 2-Heremans-Schmid glycoprotein/fetuin-A is a systemically acting inhibitor of ectopic calcification. *J. Clin. Invest.* **112**:357–366 (2003).
25. H. Hirabayashi, T. Sawamoto, J. Fujisaki, Y. Tokunaga, S. Kimura, and T. Hata. Dose-dependent pharmacokinetics and disposition of bisphosphonic prodrug of diclofenac based on osteotropic drug delivery system (ODDS). *Biopharm. Drug Dispos.* **23**:307–315 (2002).
26. H. Chen, M. Banaszak Holl, B. G. Orr, I. Majoros, and B. H. Clarkson. Interaction of dendrimers (artificial proteins) with biological hydroxyapatite crystals. *J. Dent. Res.* **82**:443–448 (2003).
27. M. J. Gorbunoff. The interaction of proteins with hydroxyapatite. II. Role of acidic and basic groups. *Anal. Biochem.* **136**:433–439 (1984).
28. H. Uludag, D. D'Augusta, J. Golden, J. Li, G. Timony, R. Riedel, and J. M. Wozney. Implantation of recombinant human bone morphogenetic proteins with biomaterial carriers: a correlation between protein pharmacokinetics and osteoinduction in the rat ectopic model. *J. Biomed. Mater. Res.* **50**:227–238 (2000).